Nuclear Engineering and Technology 52 (2020) 178–184

Contents lists available at ScienceDirect

Nuclear Engineering and Technology

journal homepage: www.elsevier.com/locate/net

Original Article

# Study on the design and experimental verification of multilayer radiation shield against mixed neutrons and γ-rays

Guang Hu [a], Huasi Hu [a, *], Quanzhan Yang [b], Bo Yu [b, **], Weiqiang Sun [a]

[a] Xi'an Jiaotong University, Xi'an, 710049, China
[b] State Key Laboratory of Light Alloy Foundry Technology for High-end Equipment Shenyang Research Institute of Foundry Co. Ltd, Shenyang, 110022, China

ARTICLE INFO

*Article history:*
Received 23 January 2019
Received in revised form
11 July 2019
Accepted 15 July 2019
Available online 16 July 2019

*Keywords:*
Optimal design
Radiation shielding
Mixed neutrons and γ-rays
Structure
Component

ABSTRACT

The traditional methods for radiation shield design always only focus on either the structure or the components of the shields rather than both of them at the same time, which largely affects the shielding performance of the facilities, so in this paper, a novel method for designing the structure and components of shields simultaneously is put forward to enhance the shielding ability. The method is developed by using the genetic algorithm (GA) and the MCNP software. In the research, six types of shielding materials with different combinations of elements such as polyethylene (PE), lead (Pb) and Boron compounds are applied to the radiation shield design, and the performance of each material is analyzed and compared. Then two typical materials are selected based on the experiment result of the six samples, which are later verified by the Compact Accelerator Neutron Source (CANS) facility. By using this method, the optimal result can be reached rapidly, and since the design progress is semi-automatic for most procedures are completed by computer, the method saves time and improves accuracy.


## 1. Introduction

It is known that neutrons and γ-rays are two main types of radiation, and in order to shield them, nuclear facilities such as accelerator neutron sources and nuclear reactors have to be carefully developed. Nowadays, commonly used shielding materials for nuclear facilities are often composed of hydrogen, heavy metal elements, neutron absorbers, and an effective shield is always multilayer. In the early stage of shield design, the concept of super shield was proposed by JaeSub Hong [1]. The shield contains three layers: a moderator that reduces the energy of the neutrons, an absorber that stops the degraded neutrons and the last layer that absorbs the γ-rays, and the super shield is constructed in accordance with the characteristics of neutrons and γ-rays, which allows each layer to perform its function in the shielding at its best. It can be seen that a multilayer radiation shield with an optimal combination of structure parameters can improve the shielding performance, otherwise, the result may deteriorate.

In order to design the optimal multilayer shield, nuclear particle transport based software MCNP is widely used. J. C. Liu adopted MCNP to design the thickness and the cost of a shield for a 14 MeV neutron source [2]. In A. X. da Silva's investigation, a shield was designed against neutrons and γ-rays for a $^{252}$Cf source through Monte Carlo simulation [3]. Also, Huasi Hu proposed a shield design method which was established by GA and MCNP software in 2008 [4], and in 2017, this method was applied to the shield design for the target station of the RIKEN Accelerator Compact Neutron Source [5]. In 2010, S Ashayer proposed a multi-objective γ-ray shielding material design method by using GA and MCNP Code, aiming at improving shielding performance and reducing the cost of shields [6]. In 2017, Mehmet Türkmen used GA and MCNP to shape the beams of neutron sources [7]. In the same year, Seyed Mehrdad also used GA and MCNP to investigate the effects of some important parameters of HPGe detector [8]. In these previous studies, either the thickness of each layer or the mass ratio of each components of a radiation shield was designed; however, they didn't devise the both at the same time, and the shields' performance was not satisfactory.

When developing a nuclear device, the shield always takes up most of the volume and weight of the nuclear device. The optimal design of the structure and components of the shield can make it much more compact and lightweight so that the efficiency of the device can be improved. Therefore, a novel method for designing the structure and components of radiation shields simultaneously is established in this research, and the shielding ability of the

* Corresponding author.
** Corresponding author.
*E-mail addresses:* huasi_hu@mail.xjtu.edu.cn (H. Hu), yub@chinasrif.com (B. Yu).

https://doi.org/10.1016/j.net.2019.07.016

materials designed by using the method is also verified by the Compact Accelerator Neutron Source (CANS) facility.

## 2. Materials and methods

### 2.1. Physical basis for the method

The purpose of shielding is to protect people from being radiated by reducing the energy of particles, absorbing the particles and their secondary radiation as much as possible. For fast neutron shielding, the interactions between neutrons and target nucleus can be divided into inelastic scattering, elastic scattering, absorption and capture. The inelastic scattering dominates in fast neutron range (around 1.0 MeV) and the elastic scattering dominates in medium energy range (around $10^{-5}$MeV–1.0 MeV). The energy of fast neutrons is mainly reduced by inelastic scattering and when the fast neutron energy drops below the threshold value of the inelastic scattering, the neutrons are slowed down by the elastic scattering until the energy of the neutrons reach the thermal neutron region. Then the thermal neutrons could be absorbed easily. For γ-rays, the shielding mainly depends on γ-rays' three forms of interactions with the shielding material: photoelectric absorption, Compton scattering and pair production. Therefore, the radiation shield has to be designed according to the interactions of neutrons and γ-rays with the material. When the energy of neutrons is high, the elements of the high inelastic cross section are chosen as the first layer, such as W, Pb, Fe and Cu. When the energy of the neutrons reaches the threshold value, the elements of the high elastic cross section are chosen as the second layer, such as H and C. The elements, B, Li and Gd of the high thermal neutron capture cross section are selected as the third layer. Commonly, the second layer and the third layer are mixed to constitute a composite material consisting of elements such as Boron carbide ($B_4C$) and PE. Secondary γ-rays are produced when neutrons interact with the material; therefore, the material consisting of W or Pb is chosen as the fourth layer for shielding the primary γ-rays and secondary γ-rays. The whole interactive process is shown in Fig. 1. The energy of neutrons is reduced after it interacts with the elements in the material, and for the shielding material as a whole, the reduced energy is closely connected with the structure and components of the material.

### 2.2. Materials for shield design

Three components PE, $B_4C$ and Pb are combined in six different groups to construct six types of shielding materials as shown in Fig. 2. In each group, the total thickness of the designed shield is 20 cm. The detector for measuring the total dose of the neutrons and γ-rays is installed on the right-hand surface of each shielding material. The area of the detector's cross section is as same as that of the shielding. The details of each group of the materials are described as follows:

- o Group (a) is a single-layer material consisting of PE, $B_4C$ and Pb.
- o Group (b) is a three-layer material with PE, $B_4C$ and Pb from left to right.
- o Group (c) is a four-layer material withPb, PE, $B_4C$ and Pb from left to right.
- o Group (d) is also a four-layer material with Pb, $B_4C$, PE and Pb from left to right.
- o Group (e) is a three-layer material with Pb, mixed material and Pb from left to right. The mixed material is made up of PE and $B_4C$.
- o Group (f) is a three-layer mixed material. Each layer consists of PE, $B_4C$, Pb.

It is worth noticing that how the six groups are designed is different:

- o The group (a): only the components of the material are well designed.
- o The group (b), (c) and (d): only the thickness ratio of each layer is well designed.
- o The group (f): the thickness of each layer and the components of the material in each layer are both well designed.

### 2.3. Computer program based on genetic algorithm and MCNP code

The design method in this research is established by using Genetic Algorithm (GA) and the MCNP Code. The parameters, such as the thickness, density and components of shielding material, are set in cell cards and material cards in MCNP code. The data showing the dose equivalent of neutrons and γ rays are extracted from the output file of the MCNP code, which are then set as the objective function of GA. In the GA program, the optimal combination of structure, components and density are sought out, which meets a preset objective. In the shielding design, the objective is the lowest dose equivalent of neutrons and γ-rays after they penetrate the shielding. The objective function is as follows:

$$\mathrm{Min}H\,(L,A) = \min[\alpha H_n(L,A) + \beta H_\gamma(L,A)] \tag{1}$$

where, $H_n(L,A)$ and $H_\gamma(L,A)$ are dose equivalents of neutrons and γ-rays respectively. In the manuscript the optimization constraint is only on the total dose equivalent. $L$ is the parameter of thickness, $A$

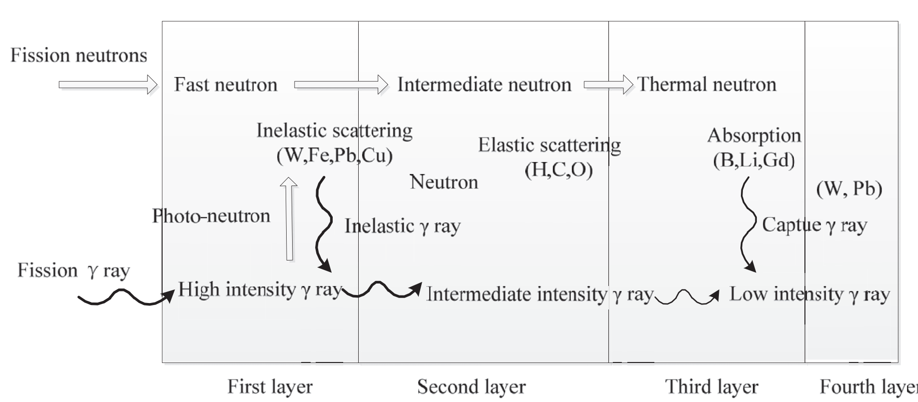


**Fig. 1.** The interactions of neutrons and γ-rays in the multilayer shield.

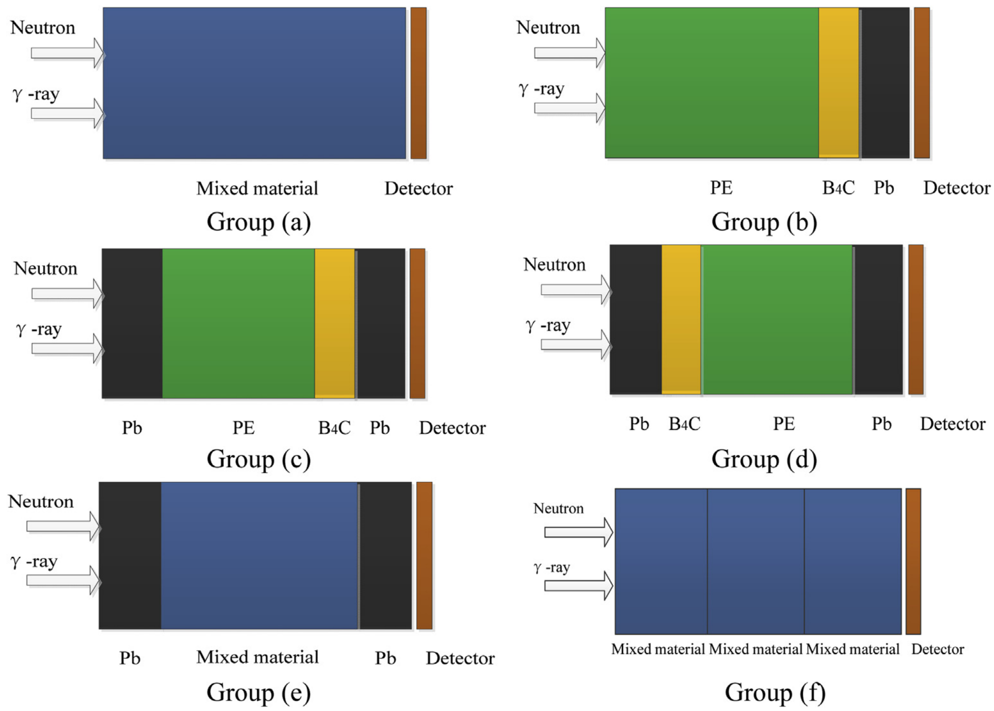


**Fig. 2.** Six groups of the shielding materials.

is the parameter of the components, $\alpha$ is the number of the neutrons and $\beta$ is the number of the $\gamma$-rays at the initial state. The constraint conditions are as follows:

$$\sum_{i=1}^{p} \frac{L_i}{L_{all}} = 1 \tag{2}$$

$$\sum_{i=1}^{p} A_1 + A_2 + \cdots A_i = 1 \tag{3}$$

$$\rho_x \leq \rho_{eff} \leq \rho_y \tag{4}$$

where, $L_i$ is the thickness of each layer, $L_{all}$ is the total thickness of the shield, $A_i$ is the mass ratio of each component and $\rho_{eff}$ is the equivalent density of the shielding.

Then, a program is written in C language to combine GA with MCNP to design the shielding material. The flow chart is shown in Fig. 3 which contains five steps as follows:

1) Input the parameters of the thickness and the components of the material.
2) Generate the "inpn" file and "inpp" file for simulating the neutrons and $\gamma$-ray passing through the material.
3) Calculate the "inpn" file and "inpp" file by MCNP and generate the "outpn" file and "outpp".
4) Extract the data for the dose equivalent of the neutrons in the "outpn" file and $\gamma$-rays in the "outpp" file.
5) The program stops when the fitness value does not change or the iteration times reach $N_0$ (the generation number). If this doesn't happen, new thickness and components of the shielding material will be generated and then the next calculation starts.

At first, MCNP model is prepared and put into the GA code. Then an executable file is produced. Double click this file, the design will begin as shown in Fig. 3, the following procedures are automatic.

This method can seek out the optimal combinations of the structures and components of the shield accurately and quickly. After MCNP model prepared and put into GA code, all the step is automatic. Even if the source is complex neutron and gamma ray spectrums, this method is also active.

## 3. Results and discussions

### 3.1. Simulation results

In this new method, the optimal combination of thickness and components is provided by the function of GA. After repeated generations' calculations of GA and with the help of MCNP, the total dose equivalent of neutrons and $\gamma$-rays reaches the minimum on the whole. Fig. 4 shows the relationship between them.

The radiation source is the fission neutrons and fission $\gamma$-rays. In one-time fission, 2.4 neutrons and 7.7 $\gamma$-rays are produced, so $\alpha$ is 2.4 and $\beta$ is 7.7 in Formula (1). The crossover rate and mutation rate in GA are both 0.3. The population size is 200 and the generation number is 500. The densities of Pb, PE, and $B_4C$ are respectively 11.34 g cm$^{-3}$, 0.96 g cm$^{-3}$ and 2.52 g cm$^{-3}$.

The design results are shown in Table 1 and Table 2.

The shielding performances of the designed materials are shown in Table 3.

From the result shown in Table 3, it can be found that 1) By comparing group (b) and group (d), (c), four-layer shield performs better than three-layer shield because Pb in the first layer of the four-layer shield is able to moderate high-energy neutrons by inelastic scattering; 2) by comparing group (a) and group (b), (c), (d), the evenly mixed one-layer material made in this research is better than multilayer material as shown in Fig. 2; 3) by comparing group

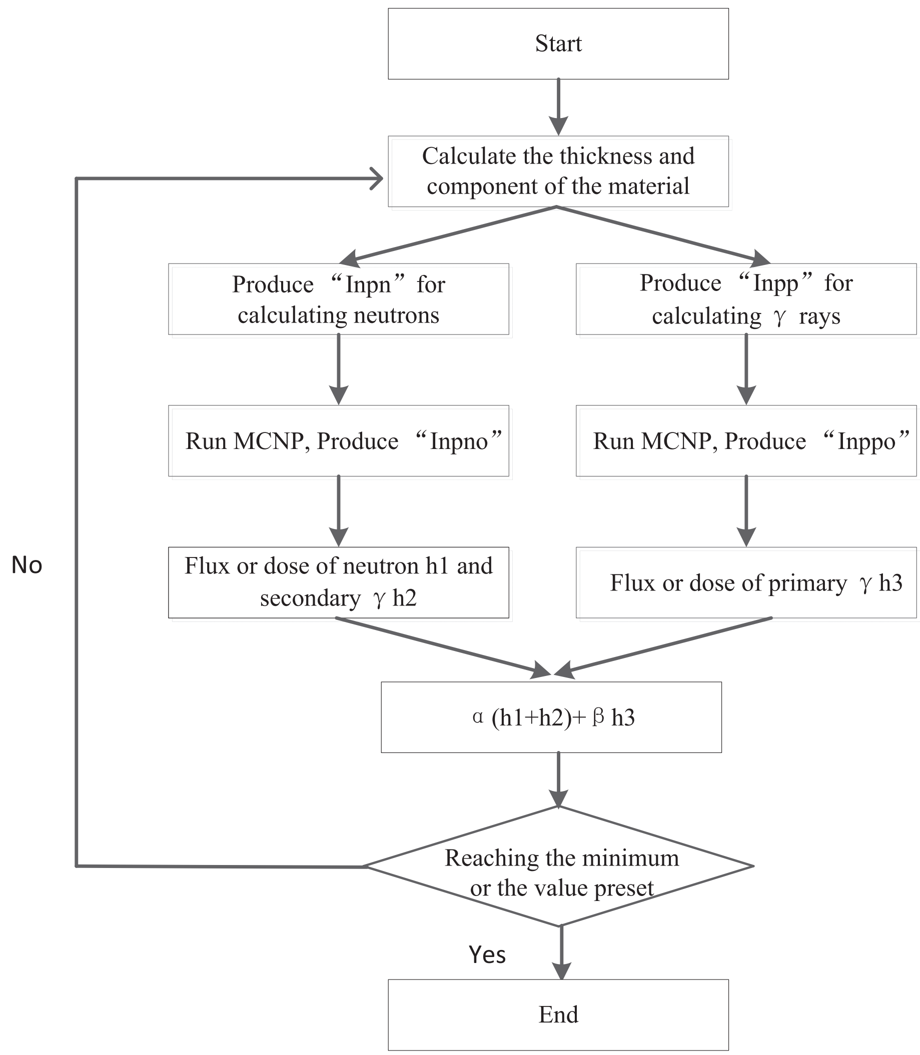


**Fig. 3.** Flow chart of the structure and components of the shield design.

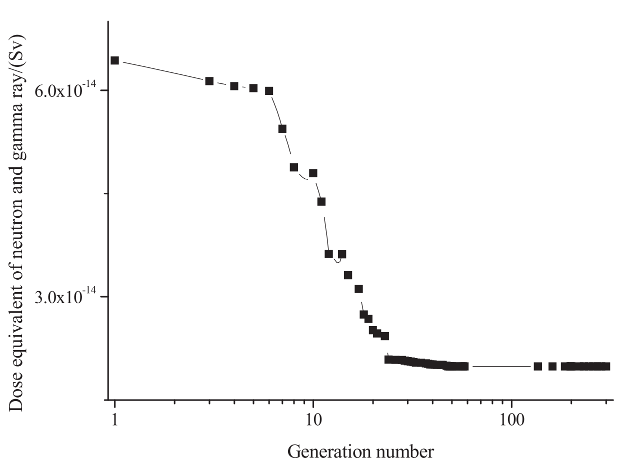


**Fig. 4.** The relationship of dose equivalent and generation number.

(e) and group (a), the material with a layout of Pb-interlayer-Pb is better than the mixed one-layer material (the interlayer is mixed by PE and $B_4C$). 4) According to group (f) and other designed shields, three-layer mixed material is better than other shields.

The designed materials are also compared with the materials made up of Pb202, Pb, Fe, graphite and Fe-PE-Pb respectively. Pb202 consists of Pb, $B_4C$ and PE. The mass ratios of Pb and PE are 80% and 19% respectively. The density of PB202 is 3.42 g $cm^{-3}$. The thickness ratio of Fe-PE-Pb is 6:3:1. Pb202 is a material with the component design only and Fe-PE-Pb with the structure design only. The shielding performances of these shields are shown in Table 4, which calculated by MCNP. The result shows that the shielding performance of group (e) and group (f) is better than that of the shield made up of pb202 and Fe-PE-Pb. But the materials with the component or structure design are better than the material without any particular design in regard to the shielding performance.

### 3.2. Experimental results

#### 3.2.1. Neutron and γ-ray spectrum of CANS

The verification experiment was carried out on the CANS. The CANS consists of a 7 MeV proton linear accelerator, a target station, a neutron beam tube and a box for experiment samples as well as the detector [9]. Two typical materials are selected for the experiment, one is PE + Pb and the other one is BPE + Pb. The structure and components of the CANS are shown in Fig. 5. Inside the graphite reflector is the beryllium target [10]. Outside the graphite

**Table 1**
The thickness of the shield's each layer.

| | No. of layers | First layer (cm) | Second layer (cm) | Third layer (cm) | Fourth layer (cm) |
|---|---|---|---|---|---|
| Group (a) | 1 | 20 | 0 | 0 | 0 |
| Group (b) | 3 | 18.10 | 0.10 | 1.80 | 0 |
| Group (c) | 4 | 2.87 | 16.45 | 0.30 | 0.38 |
| Group (d) | 4 | 2.82 | 0.52 | 16.54 | 0.12 |
| Group (e) | 3 | 2.42 | 17.54 | 0.04 | 0 |
| Group (f) | 3 | 8.46 | 0.68 | 10.86 | 0 |

**Table 2**
The components of the shield's each layer.

| | | PE (W/%) | $B_4C$ (W/%) | Pb (W/%) |
|---|---|---|---|---|
| Group (a) First layer | | 0.393 | 0.032 | 0.575 |
| Group (e) | Second layer | 0.604 | 0.092 | 0.304 |
| Group (f) | First layer | 0.175 | 0.011 | 0.814 |
| | Second layer | 0.387 | 0.001 | 0.612 |
| | Third layer | 0.514 | 0.050 | 0.436 |

**Table 3**
Comparison of shielding performances of different materials.

| | Shielding performance (Sv) | | | | Density (g.cm$^{-3}$) |
|---|---|---|---|---|---|
| | Neutron | Secondary γ | γ-ray | Total | |
| Group (a) | 1.79E-14 | 1.20E-16 | 2.85E-15 | 2.09E-14 | 2.52 |
| Group (b) | 1.96E-14 | 7.47E-16 | 3.34E-15 | 2.37E-14 | 2.11 |
| Group (c) | 1.89E-14 | 1.88E-15 | 1.98E-15 | 2.27E-14 | 1.91 |
| Group (d) | 1.93E-14 | 1.69E-15 | 1.62E-15 | 2.26E-14 | 2.65 |
| Group (e) | 1.79E-14 | 2.62E-16 | 1.70E-15 | 1.99E-14 | 2.66 |
| Group (f) | 1.76E-14 | 1.92E-16 | 1.72E-15 | 1.93E-14 | 2.63 |

**Table 4**
Comparison of shielding performances of different shields.

| | Shielding performance (Sv) | | | | Density (g.cm$^{-3}$) |
|---|---|---|---|---|---|
| | Neutron | Secondary γ | γ-ray | Total | |
| No shielding | 4.90E-13 | 0.00 E+00 | 2.34E-14 | 5.14E-13 | 0 |
| Pb | 1.69E-13 | 8.52E-17 | 1.92E-18 | 1.69E-13 | 11.3 |
| Fe | 1.32E-13 | 2.08E-16 | 5.40E-17 | 1.33E-13 | 7.86 |
| Graphite | 8.47E-14 | 6.46E-17 | 5.24E-15 | 9.00E-14 | 2.25 |
| PB 202 | 4.78E-14 | 1.04E-16 | 7.67E-16 | 4.87E-14 | 3.42 |
| Fe-PE-Pb | 3.98E-14 | 6.89E-16 | 1.20E-16 | 4.06E-14 | 6.13 |

reflector is a shield made up of PE and Pb. The collimator consists of BPE and PE. The inside layer of the collimator is BPE and the outside layer is PE. The box is made up of PE and Pb. The distance between the detector and the PE moderator is 484 cm. The size of the detector is 5.0 cm × 3.2 cm.

The simulation started with proton bombing beryllium target, which produced the neutrons and γ-rays. When the current beam of the proton was 100 μA, the total number of the neutrons and γ-rays was about 1.23X10$^{12}$/s, in which neutrons was 9.80 × 10$^{11}$/s [11]. The energy of γ-ray was 3.562 MeV [11]. The neutron spectrum and γ-ray spectrum at the detector were simulated by MCNP and PHITS. PHITS is a kind of Monte Carlo software for simulating the interaction of neutrons and γ-ray s with matters. The simulation results are shown in Fig. 6.

### 3.2.2. Experimental setup

Fig. 7 is the setup of the experiment. The detector is 484 cm away from the PE moderator. The center of the detector and the center of the neutron beam are in a straight line. The detector consists of the scintillator and the multi-pixel photo counter. The scintillator is made up of poly vinyl toluene, *p*-terpheny and POPOP. In order to avoid the dead time of the detector, the current of the proton beam in the experiment was set to be around 13.5 μA [5]. The detector can't distinguish neutrons from γ-rays, so only the total number of the neutrons and γ-rays is shown [5].

Before putting the sample into the CANS, the two typical materials which will be used in the experiment are designed by the new method. The source is shown in Fig. 6. The detailed design procedures and the design result are shown in 3.3.1. Table 5 illustrates the selected groups of components for the material design, among which 4.18 cm PE+1cmPb and 5 cm BPE+1cmPb are selected according to the design result.

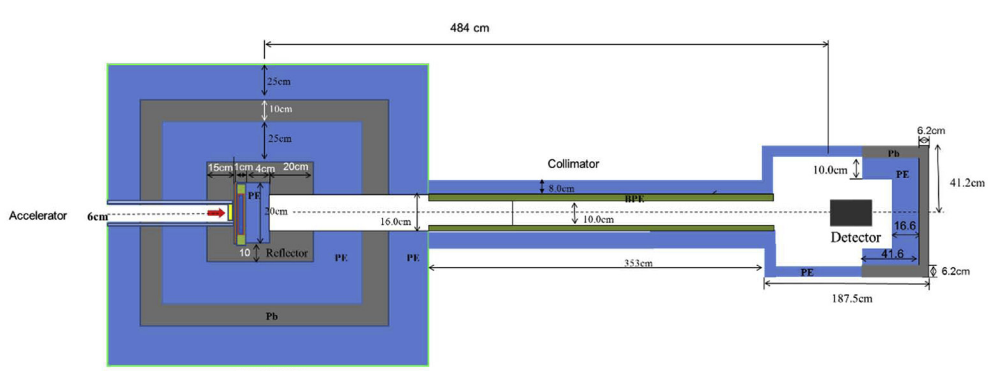


**Fig. 5.** The structure of the CANS.

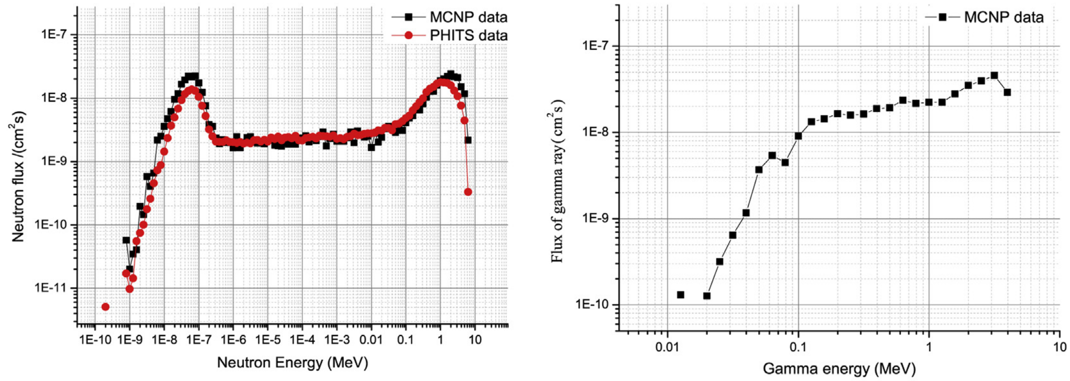


(a) Neutron spectrum (b) γ-ray spectrum

**Fig. 6.** The neutron spectrum and γ-ray spectrum at the detector.

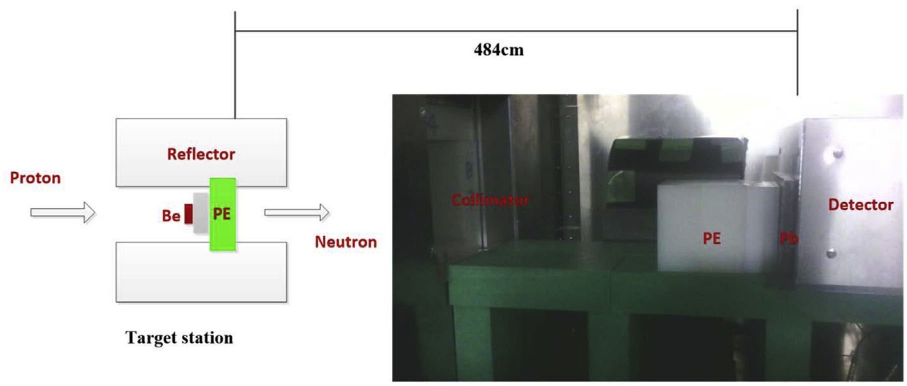


**Fig. 7.** The setup of the experiment.

### 3.2.3. Uncertainty analysis

The neutron number is proportional to the current beam of protons, the number of pulses and the measurement time. The uncertainty of the neutron number is due to the uncertainty of these measurement parameters. The uncertainty of neutron number is calculated by

$$E_N = \frac{\Delta_N}{N} = \sqrt{\left(\frac{\partial \ln f}{\partial_a}\right)^2 \Delta_a^2 + \left(\frac{\partial \ln f}{\partial_b}\right)^2 \Delta_b^2 + \left(\frac{\partial \ln f}{\partial_c}\right)^2 \Delta_c^2 + \left(\frac{\partial \ln f}{\partial_d}\right)^2 \Delta_d^2} \qquad (5)$$

where, $N$ is the neutron number, $\Delta_a$ is the uncertainty of the detector, $\Delta_b$ is the uncertainty of the current beam of protons, $\Delta_c$ is the uncertainty of the pulse number of protons, $\Delta_d$ is the uncertainty of measurement time. The relative uncertainty of the detector is calculated by

$$|\Delta N| / N = (1/N) \times 100\% \qquad (6)$$

The uncertainties of the measurement of the current beam of protons and the pulse number of protons are smaller than 2%. The measurement time is 60 ± 1.2 s.

**Table 5**
Selected groups of components for the shield design in the experiment.

| Group a with PE and Pb | | | Group b with BPE and Pb | |
|---|---|---|---|---|
| Sr. # | Thickness of PE (cm) | Thickness of Pb (cm) | Thickness of BPE (cm) | Thickness of Pb (cm) |
| 1 | 0.54 | 1 | 5 | 1 |
| 2 | 4.18 | 1 | 10 | 1 |
| 3 | 9.30 | 1 | 15 | 1 |
| 4 | 13.90 | 1 | 20 | 1 |
| 5 | 19.20 | 1 | | |

The error of the simulation is calculated by

$$\Delta_t = \sqrt{f_n^2\Delta_n^2 + f_{\gamma1}^2\Delta_{\gamma1}^2 + f_{\gamma2}^2\Delta_{\gamma2}^2} \quad (7)$$

where, $f_n$ is the flux of neutrons, $f_{\gamma1}$ is the flux of secondary γ-rays, $f_{\gamma2}$ is the flux of primary γ-rays, $\Delta_n$ is the error of neutrons, $\Delta_{\gamma1}$ is the error of secondary γ-rays, $\Delta_{\gamma2}$ is the error of primary γ-rays.

### 3.3. Comparison of simulation and experimental results

#### 3.3.1. Simulation result of the new method in response to the neutron and γ-ray spectrums of CANS

The energy and intensity of the mixed neutrons and γ-rays from the CANS are close to the fission neutrons and fission γ-rays. Therefore, the verification experiment was carried out on the CANS. The simulation starts with the neutron spectrum and γ-ray spectrum shown in Fig. 6. The structure and components are shown in Fig. 5. The position of the detector is as same as that in the experiment.

The thickness and components of PE + Pb and the BPE + Pb were well designed to shield the mixed neutrons and γ-rays shown in Fig. 6. The density of PE is 0.96 g $cm^{-3}$. BPE is a mix of PE and $B_2O_3$. The objective is to obtain the minimum quantity of neutrons and γ-rays after them penetrating the shield. The designed result is as followed: the thickness ratio of PE and Pb is 4.2:1. The thickness of BPE and Pb is 4.96:1. The mass ratio of $B_2O_3$ is 9.6% in BPE.

The simulation result is shown in Fig. 8. It is the transmission ratio of both neutrons and γ-rays. The γ-rays include the primary γ-rays and secondary γ-rays produced by the interaction of neutrons and the shielding material.

#### 3.3.2. Comparison and analyses

Fig. 8 is the experimental data and the simulated data of different shields. The abscissa shows the thickness of the shield as a whole. The ordinate illustrates the transmission ratio of both neutrons and γ-rays. As the thickness increases, the transmission ratio decreases. The groups of 4.2 cm PE + 1 cm Pb and 5 cm BPE + 1 cm Pb, which are arranged according to the designed result, are able to shield more neutrons and γ-rays than other combinations of components adopted to make other kinds of shields. 5 cm BPE + 1 cm Pb sample whose structure and components were designed at the same time shields more neutrons and γ-rays than 4.2 cm PE + 1 cm Pb whose structure was the only concern while being designed.

To sum up, the shield with only structure or components designed reduces more neutrons and γ rays than other shields with no particular design. The shield with structure and components designed together reduces more neutrons and γ-rays than the shield with only structure or components designed.

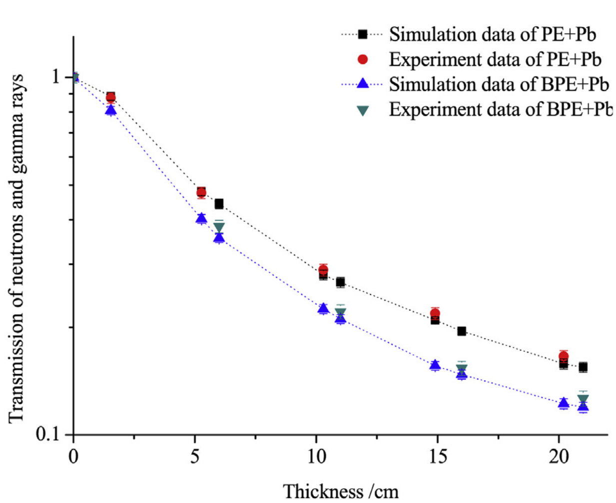


**Fig. 8.** The experimental data and simulated data of different shields.

## 4. Conclusions

The novel method is suitable for designing both the structure and components of a shield against arbitrary mixed neutrons and γ-rays. The shield designed by this method is better than other shields in terms of radiation resistance. The research also shows that the one-layer evenly mixed shield is better than some multilayer shields, but the Pb-interlayer-Pb shield is better than other shields except for the layer mixed shielding which is the best among all. The verification experiment was carried out on the CANS, in which PE + Pb and BPE + Pb were selected as the sample materials. The thickness ratios and components of these materials are designed against the mixed neutrons and γ-rays generated from the CANS. The selected groups of components adopted to make the shield, which are arranged according to the designed results, are able to shield more neutrons and γ-rays than other groups. A 5 cm BPE + 1 cm Pb sample, whose structure and components were designed at the same time, shields more neutrons and γ rays than a 5.18 cm PE + 1 cm Pb sample whose structure was only predesigned.

## Acknowledgments

This research is supported by the NSAF Joint Fund set up by the National Natural Science Foundation of China and the Chinese Academy of Engineering Physics under Grant (U1830128), State Key Laboratory of Light Alloy Foundry Technology for High-end Equipment (No. LACT-001), Postdoctoral Science Foundation of China (2018M633521), Nature Science foundation of Liaoning Province of China (No. 20180550876) and International Project for Associates (IPA) of Riken in Japan. Many thanks go to the members of the neutron beam team in Riken for assistance with the simulation and the experiment.

## Appendix A. Supplementary data

Supplementary data to this article can be found online at https://doi.org/10.1016/j.net.2019.07.016.

## References

[1] JaeSub Hong, Development of neutron shielding for gamma-ray telescopes in space and observation of galactic center sources by a balloon-borne gamma-ray telescope, UMI (2002) 54–57. Number: 3037716.
[2] J.C. Liu, T.T. Ng, Monte Carlo calculations using MCNP4B for an optimal shielding design for a 14 MeV neutron source, Radiat. Prot. Dosim. 83 (3) (1999) 257–262.
[3] A.X. da Silva, V.R. Crispim, Shielding design studies for a neutron irradiator system based on a 252Cf source, Radiat. Prot. Dosim. 95 (4) (2001) 333–338.
[4] Huasi Hu, Qunshu Wang, Juan Qin, et al., Study on composite material for shielding mixed neutron and γ –rays, IEEE Trans. Nucl. Sci. 55 (4) (2008) 2376–2384.
[5] Guang hu, Huasi Hu, et al., New shielding material development for compact neutron source, AIP Adv. 7 (4) (2017) 324–341.
[6] Sahar Ashayer, Mansur Asgari, Hossein Afarideh, Optimizing gamma-ray shielding material by using genetic algorithm and MCNP code, ICONE18-29018 (2010) 325–328.
[7] Mehmet Türkmen, Şule Ergün, Üner Çolak, A new method in beam shaping: multi-Objective Genetic Algorithm method coupled with a Monte-Carlo based reactor physics code, Prog. Nucl. Energy 99 (2017) 165–176.
[8] Seyed Mehrdad, Zamzamian Seyed, Abolfazl Hosseini, Optimization of the marinelli beaker dimensions using genetic algorithm, J. Environ. Radioact. 172 (2017) 81–88.
[9] Otake Yoshie, RIKEN compact neutron systems with fast and slow neutrons, Plasma Fusion Res. 13 (2018) 2401017.
[10] Y. Yamagata et al, PCT/HP2013/056188.
[11] W.B. Howard, et al., Measurement of the thick-target $^{9}Be$ (p, n) neutron energy spectra, Nucl. Sci. Eng. 138 (2) (2015) 145–160.